Sensors and Actuators B 250 (2017) 420–428

Contents lists available at ScienceDirect

Sensors and Actuators B: Chemical

journal homepage: www.elsevier.com/locate/snb

# Strategies for fabrication of highly-dense ordered arrays of metal microdisks by the scanning electrochemical microscopy microwriting approach

Mariela A. Brites Helú, José L. Fernández *

*Instituto de Química Aplicada del Litoral (IQAL) and Programa de Electroquímica Aplicada e Ingeniería Electroquímica (PRELINE), Facultad de Ingeniería Química, Universidad Nacional del Litoral, Santiago del Estero 2829, S3000AOM Santa Fe, Santa Fe, Argentina*

ARTICLE INFO

*Article history:*
Received 24 January 2017
Received in revised form 7 April 2017
Accepted 24 April 2017
Available online 29 April 2017

*Keywords:*
Microelectrode arrays
Micro-patterning
Scanning electrochemical microscopy
Recessed microelectrodes
Electrodeposition

ABSTRACT

The microwriting approach of the scanning electrochemical microscopy (SECM) was adapted and optimized for the fabrication of extensive ordered arrays of gold microdisks deposited on conductive supports. This technique uses a SECM tip as a source for the localized delivery of metal ions by well-controlled electro-dissolution of the metal microelectrode. In this work, novel configurations of recessed-microelectrode tips (radii $\leq$ 12.5 μm) were developed to make possible the deposition of a large number of well-defined disks from the same probe by a semi-automatic procedure. A sequence of steps that coordinates tip potential, tip position, and substrate potential values was designed and implemented to improve the repeatability and confinement of the deposited microdisks. The effects of potential and time conditions for gold electro-dissolution and electrodeposition on the morphological properties of gold disks deposited on Pt and glassy carbon were explored. The selective modification of glassy carbon-supported gold arrays with an electrocatalytic material (Pt) for a specific reaction (hydrogen evolution) and their further SECM activity screening were described to illustrate a way to use them as multielectrode platforms.



## 1. Introduction

Ordered arrays of microelectrodes with varied shapes and sizes are electrode platforms with applications in fundamental and applied areas of chemistry. These are valuable configurations for applications in sensors [1,2–4], micro-batteries [5,6], activity screening of electro- and photo-catalytic materials [7,8], as well as in fundamental studies of mass transport phenomena [9,10] and of synergetic effects in electrocatalysis [11], among many other uses. In these platforms the microelectrodes can be either individually connected [3,4,12,13], or wired by a single connection through a common conductive support [7,8,11,14–16]. Many of the potential applications of these arrays entail a large number (or a high density) of microelectrodes. Thus, most of the methods used for fabrication of arrays rely on lithographic and microfabrication techniques [3–6,12–16] that in most cases require specific facilities.

Microfabrication methods based on localized electrochemical deposition of materials have the advantage to require relatively simple instrumentation. Besides, they have great potentiality to push the resolution of microfabrication techniques to the sub-micrometer and nanometer levels [17,18]. Localized electrodeposition can be attained by coupling electrochemical methods with micro-positioning devices [19–21], for example with the scanning electrochemical microscopy (SECM), which was one of the pioneering techniques of this type [22]. SECM offers nowadays a variety of operation modes to tackle situations with diverse requirements of resolution, size, shape, and material nature [23]. In general, SECM-based patterning methods use the SECM probe to induce localized delivering or etching of materials [23–25]. In most cases the whole substrate is polarized, so localization of the patterning process on the substrate is mainly governed by the radial distribution of tip-generated reactant concentration between the tip and the substrate. Then, not only the tip size but also the distance between the tip and the substrate (absolute value and constancy along the pattern) are critical parameters that limit the resolution and extension of the patterns. Among the different operation modes, the so-called "microwriting" method developed by Meltzer and Mandler [25] is a simple and versatile procedure with potential application in a great number of microfabrication processes. This approach relies on the electrochemical [24–26,27] or chemical [28,29] deposition

* Corresponding author.
*E-mail address:* jlfernan@fiq.unl.edu.ar (J.L. Fernández).

http://dx.doi.org/10.1016/j.snb.2017.04.155
0925-4005/

of a metal on the substrate surface from metal ions that are locally electro-dissolved at the metallic tip. When the transfer of material from the tip to the substrate is coordinated with the tip movement, arrays of metallic disks or bands can be obtained [23–29].

While the SECM microwriting approach should be potentially useful for fabrication of microelectrode arrays, its implementation still requires optimization of probes and fabrication conditions that are critical for attaining a proper confinement of the deposited structures, particularly when extensive arrays with high density of microelectrodes are required. For that reason the method was never applied beyond a demonstrative proof of concept with small arrays. Thus, the goal of the present work is to expand the application of the microwriting SECM-based technology to the fabrication of highly-dense arrays of disk microelectrodes, by developing both new types of probes and fabrication programs that assure a proper control of dissolution/deposition potentials, times and confinement. Moreover, in order to exemplify potential uses of these high-density arrays, this work demonstrates a possible way to modify them for their use as platforms supporting an electrocatalytic material with a specific function.

## 2. Materials and methods

### 2.1. Chemicals and materials

Analytical grade copper sulphate, sulphuric acid (98%), and hydrochloric acid (35%) from Merck (Germany) and hexachloroplatinic(IV) acid hydrate from Aldrich (USA) were used as received. Water was deionized with an exchange resin, doubly distilled, and treated with a Purelab purifier (Elga Labwater, resistivity ≥18.2 MΩ cm). Array supports were glassy carbon plates (1 mm thick, type I) from Alfa Aesar (USA) and platinum foils (0.3 mm thick) from Vega & Camji (Argentina), which were polished with alumina powder and ultrasonically cleaned in water. High purity wires of Pt from Alfa Aesar (USA) and of Au from Goodfellow (UK), and borosilicate glass capillaries (1.5 mm outer diameter, 0.1 mm thickness) from Paralwall (Argentina) were employed for fabrication of SECM probes.

### 2.2. Instrumentation

For a visual inspection of tips and arrays an optical microscope (Nikon Optiphot with a FX-35DX camera) was used. The morphology and composition of the arrays were characterized by SEM using a benchtop scanning electron microscope PhenomWorld model PROX (Netherlands) equipped with an energy dispersive X-ray spectrometer (EDS), and by AFM in contact mode using a scanning probe microscope Agilent 5400 (USA). The mechanical stability was evaluated by mounting the arrays on the Teflon tip of a rotating disk electrode (RDE) Radiometer EDI 10 K (France). Array fabrication and scanning electrochemical microscopy experiments were carried out using a home-built SECM instrument described elsewhere [30], furnished with a bipotentiostat Heka Elektronik (Germany) model PG340. The tip position was controlled with three motorized translation stages Zaber model T-LS (Canada) with 28 mm travel distance, and a XYZ nanopositioning system Physik Instrumente (Germany) model Nanocube P-611.3S. Both the bipotentiostat and the positioning systems were commanded by the software Potmaster (Heka Elektronik) batch-controlled via LabView programs (National Instruments, USA). The SECM Teflon cell had a typical configuration, with a platinum wire (Vega & Camji) as counter-electrode and a SECM tip as working electrode. The reference electrodes were a saturated calomel electrode (SCE) for experiments in HCl and in Cu-containing solutions, and a reversible hydrogen electrode (RHE) for SECM evaluation of the hydrogen evolution reaction. The SECM cell was supported on a flat platform that allowed tilt correction via two graduated micrometer screws, which is critical for the reproducibility of the tip-substrate distance during the fabrication sequence.

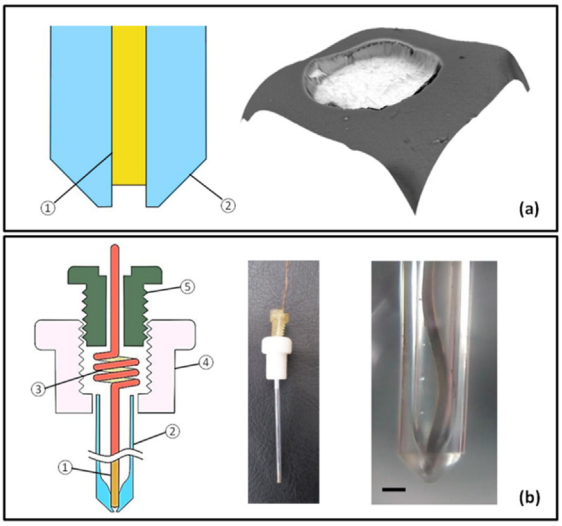


**Fig. 1.** (a) Scheme (left) and 3D-reconstruction of a SEM image (right) of a 25-μm-diameter Au RDP-A probe. (1) Sealed and etched Au wire leaving a recessed disk; (2) polished and sharpened sealing capillary. (b) Scheme (left) and photograph (center) of the RDP-B probe. (1) Au wire; (2) glass micropipette; (3) copper wire and spring; (4) threaded nipple; (5) pushing screw. The optical micrograph at the right shows the Au wire pushed against the pipette cavity at the bottom (scale bar: 500 μm).

### 2.3. Fabrication of SECM tips for micro-patterning

The proposed micro-patterning method relies on the ability to transfer a "slice" of metal from the microelectrode to its projected area onto the substrate surface by a mechanism involving electro-dissolution, mass transport and electro-deposition. In order to make this sequence to work efficiently, diffusion of the dissolved metal ions toward the bulk solution must be avoided. This can be attained by confining the transfer sequence into a small gap between microelectrode and substrate surfaces, either by working with a conventional disk microelectrode tip in very close proximity to the substrate [25,27,28] or by using a tip configuration with the microelectrode surface slightly recessed below the glass sheath surface. By following this last way, a recessed tip can be approached until its sheath surface makes contact with the substrate surface, building a cylindrical microcell laterally limited by the glass sheath walls where the metal transfer can proceed in a confined and quasi-isolated environment. Thus, to apply this strategy in this work, recessed-disk gold microelectrodes were used as SECM tip for fabrication of gold microdisk arrays by the microwriting method. Two configurations of recessed-disk probes were evaluated seeking to obtain more extensive and better defined arrays. Simple schemes of these two configurations are shown in Fig. 1.

The recessed-disk probe A (RDP-A), schematized in Fig. 1a, was fabricated by heat-sealing of Au wires into borosilicate glass capillaries, polishing and sharpening [31] to obtain Au disk tips, followed by a short electrochemical etching. First, pieces of 25-μm-diameter Au wires were soldered to copper wires using a micropoint soldering machine (S&H Dental, Argentina) and introduced into borosilicate glass capillaries. Then, their ends were melted by careful heating under a torch flame until the sealing of about 2 mm of the wires was visually verified. The capillaries were polished with coarse sandpaper until the cross section of the wire was exposed. A final polishing with an increasing-grit

sequence of sandpapers and 0.3-μm alumina slurry was applied to finish the surface. The glass wall surrounding the gold disk was also conically sharpened by mechanical polishing to reach *Rg* values not larger than 3 (where *Rg* = tip radius/disk radius [30]). In order to obtain a recessed tip, the exposed 25-μm-diameter Au disk was electrochemically etched in 0.1 M HCl by applying an oxidative potential (0.5–0.6 V) during 4 min against a gold wire counter-electrode placed at 1 cm from the tip end. As it is observed in the micrograph of Fig. 1a, a cavity with a deepness of 3–4 μm was obtained. The recessed tips were finally rinsed and sonicated for more than 5 min with ultrapure water, dried and stored in air.

The other tested configuration, the recessed-disk probe B (RDP-B) schematized in Fig. 1b, is in fact a micropipette able to accommodate and fit the end of a gold wire just on top of its opening. These micropipettes can be fabricated by the usual heat-pulling procedures [32], but in this work they were made by heat-sealing of a sharpened gold wire into the very end of a capillary and removing it to leave a conical inner space just over the pipette opening. In order to fabricate these micropipettes, 250-μm-diameter Au wires were soldered to copper wires and sharpened by electropolishing in concentrated HCl as it is usually done for preparing Au STM tips [33]. The sharpened Au wires were heat-sealed into the end of a borosilicate glass capillary, and polished until the Au wire cross section with the desired diameter (around 25 μm) was exposed. The glass sheath surrounding the gold disk was then polished to decrease the probe *Rg* to values smaller than 3. Next, the sealed Au cone was totally dissolved by electrochemical etching as it was previously described for fabrication of RDP-A probes. Once the wire slackened off, it was removed from the capillary leaving a conical cavity with a deepness smaller than 100 μm. The resulting micropipette was cleaned in *aqua regia* to eliminate residual Au, rinsed with ultrapure water and dried in hot air. As it is schematized in Fig. 1b, the pipette upper end was press fitted into a hole at the bottom of a cylindrical Teflon holder that had an inner thread at the opposite side. Another 250-μm-diameter gold wire was welded to a copper wire with a spring at its end, placed inside the micropipette, and tightened by a plastic screw through the Teflon thread, ensuring a good seat of the Au wire end against the pipette inner conical wall (as it is shown in the optical micrographs of Fig. 1b).

### 2.4. Fabrication of disk arrays by SECM microwriting

The proposed method has its bases on the general SECM microwriting procedure well described elsewhere [25–28], but it incorporates variants in the employed probes (as described in the previous section) and in the sequence of steps designed for semi-automatic fabrication. Gold microdisk arrays were fabricated using a typical 4-electrode SECM cell. On the one hand, the RDP-A probes were approached in 0.1 M HCl solution sensing the limiting current for the reduction of dissolved oxygen at 0 V vs. SCE, using the negative feedback caused by the substrate proximity [7] to detect the position of contact between tip and substrate [34]. On the other hand, the RDP-B probes containing the wire were filled with HCl solution just in the conical reservoir and approached to the substrate in air (while applying 0.5 V between them). The approach end point was identified by detecting the current that started to flow between the tip and the substrate when the tip arrived the substrate surface and the circuit was closed by the electrolyte solution. Then the cell was filled with 0.1 M HCl solution. Once either of these probes was in contact with the substrate, it was withdrawn a distance $Z_w$ (typically $Z_w$ = 300 μm), placed at the array initial position ($X_i$, $Y_i$), and the sequence for the array fabrication started (which was identical for both tip configurations). For example, for fabrication of a square array with aligned columns and rows of disks, this sequence is schematized in Fig. 2. Initially, both the tip and the substrate were held at neutral potentials $E_{T,n}$ and $E_{S,n}$, respectively, where no reactions proceeded on both electrodes ($E_{T,n}$ = 0 V and $E_{S,n}$ = 0.1 V vs. SCE). As a first step, after re-approaching the tip, the transfer of a metal slice from the probe to the substrate was initiated. An important detail was to introduce a rest time $t_R$ of 1 s after positioning the tip on the desired place to ensure a quiet environment during the metal transfer. An anodic potential $E_{T,dis}$ was then applied to the tip to oxidize metallic Au to Au(III) and dissolve it as $AuCl_4^-$ [26] (typically $E_{T,dis}$ = 1.04–1.1 V vs. SCE). Simultaneously, a cathodic potential $E_{S,dep}$ was applied to the substrate to electroreduce the tip-generated Au ions under diffusion control ($E_{S,dep}$ was −0.2 V and −0.3 V vs. SCE for Pt and GC substrates, respectively). These conditions were kept for a deposition time $t_{dis}$ = 2–4 s, and then the probe potential was changed to $E_{T,n}$ while keeping the substrate potential at $E_{S,dep}$ to complete a deposition time $t_{dep}$ about twice $t_{dis}$. A $t_{dep}$ value larger than $t_{dis}$ was applied to ensure that all the dissolved Au at the cavity was electrodeposited on the substrate before withdrawing the tip to move it to a new position. Then $E_S$ was also changed to $E_{S,n}$ and the translation of the tip to the new position was started. For this movement, the tip was lifted a distance $Z_w$, moved the desired $\Delta X$ distance over the $X$ axis, and approached again onto the new position. Even though $E_S$ could be kept invariant at the $E_{S,dep}$ value during the whole sequence, it was verified that during steps where the tip moves the solution becomes agitated, and mass transport of impurities toward the substrate by convection becomes important. Then, changing $E_S$ to a value where no deposition should occur ($E_{S,n}$) during moving the tip is a safe procedure to diminish undesired electrodeposition of impurities on the substrate. This deposition-translation sequence was controlled and repeated by a LabView program until the row was complete. Then the tip was moved the desired $\Delta Y$ distance over the $Y$ axis and translated to the initial $X_i$ coordinate to initiate a new row following the same sequence. Diverse arrangements, not necessarily square or symmetric, could be fabricated by applying the described sequence following a software-predefined pattern across the surface.

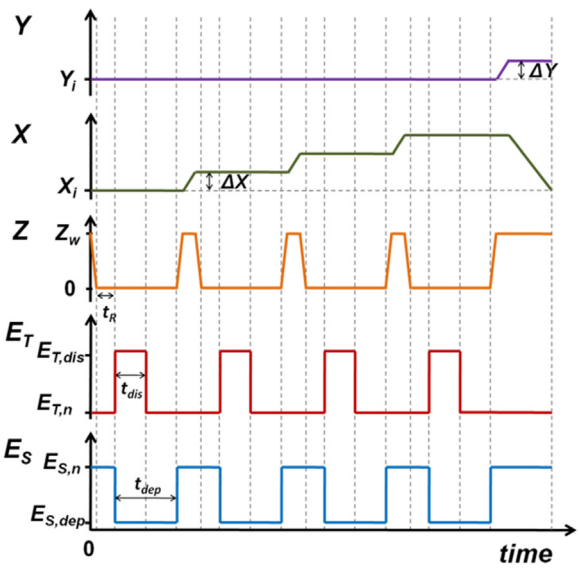


**Fig. 2.** Sequence of steps to fabricate a single row of disks by the SECM microwriting approach. This sequence was repeated according to the number of rows in the array.

### 2.5. Analysis of mechanical stability by a hydrodynamic test

In order to evaluate the stability of electrodeposited Au microdisks against mechanical perturbations, the arrays were subjected to strong hydrodynamic tensions generated in typical RDE experiments. Au-disk arrays supported on glassy carbon and on

platinum were mounted on a RDE tip masking the support with adhesive Teflon tape (0.1 mm thickness) and leaving exposed a total circular area of ~0.8 $mm^2$ (1 mm diameter) around the array. The RDE was immersed in a 0.5 M $H_2SO_4$ solution, and rotated at 7000 rpm during 30 min. The integrity of the Au arrays deposited on Pt was evaluated by comparing the voltammetric charges of surface processes detected for Au and Pt in cyclic voltammograms (CVs) measured in 0.5 M $H_2SO_4$ solution before and after rotation over the potential range 0–1.6 V vs. RHE at 0.1 V/s. For Au microdisks deposited on glassy carbon, as the substrate oxidizes at such anodic potentials, their integrity was only evaluated by SEM inspection after the hydrodynamic experiment.

### 2.6. Modification of Au microdisk arrays with Pt

Selective modification with Pt of Au microdisk arrays deposited on glassy carbon (GC) was carried out by underpotential deposition (UPD) of Cu monolayers and further displacement of Cu by Pt following a reported procedure [35]. First the complete array was immersed in 0.05 M $CuSO_4$ + 0.5 M $H_2SO_4$ solution in a classical 3-electrode cell while holding its potential at 0.65 V vs. SCE for 20 s to ensure the surface is free of Cu. In order to produce the electroadsorption of UPD Cu, the electrode potential was scanned to the desired deposition potential ($E_{UPD}$) at the scan rate of 0.4 V/s and was held at this value during a deposition time $t_{UPD}$. The effects of $E_{UPD}$ and $t_{UPD}$ were previously explored on a gold disk microelectrode by applying different $E_{UPD}$ values for a fixed $t_{UPD}$ and a constant $E_{UPD}$ value for different $t_{UPD}$ values, respectively, and subsequent stripping of the resulting copper overlayer by linear sweep from $E_{UPD}$ to 0.65 V [35]. After this exploration, it was concluded that by using values of $E_{UPD}$ = 0.1 V vs. SCE and of $t_{UPD}$ = 120 s, a complete monolayer of Cu can be obtained. The modified array electrode was taken out from the solution without opening the cell circuit, disconnected, rinsed with tri-distilled water and immersed in 6 mM $H_2PtCl_6$ + 0.5 M $H_2SO_4$ for at least 10 min to replace Cu monolayer with Pt through redox replacement. This modification cycle was repeated 3 times to thicken the platinum deposit. The previous procedure allowed to deposit similar amounts of Pt over all the Au disks in the array.

### 2.7. SECM analysis of the hydrogen evolution reaction on Pt-modified arrays

The catalytic activity for the hydrogen evolution reaction was evaluated on Pt-modified arrays. Substrate generation-tip collection (SG-TC) screening of the activity for hydrogen evolution [36] over Pt-modified Au-disk arrays on GC was performed in 0.5 M $H_2SO_4$. A typical four-electrode SECM cell and Pt tips fabricated by the classical heat-sealing/polishing procedure [36] were employed. The Pt tip was approached over a region of the substrate close to the array using the negative feedback for reduction of dissolved oxygen [7]. Screening measurements were performed by scanning the tip at a tip-substrate distance of 30 μm, holding the substrate potential at −0.05 V vs. RHE and the tip potential at 0.4 V vs. RHE (to electrooxidize dissolved hydrogen produced on Pt). This value of $E_S$ close to the RHE potential was chosen to evolve hydrogen on Pt ad-layers without forming bubbles at a reaction rate that is very sensitive to the Pt coverage [37], so small differences should be more evident during the screening.

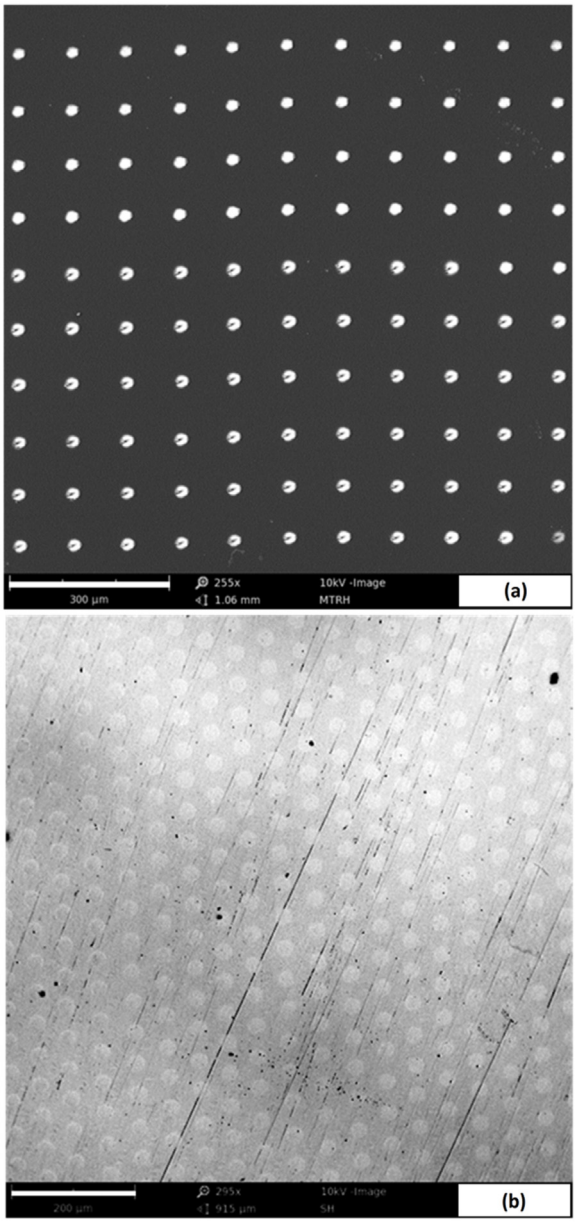


**Fig. 3.** SEM backscattered-electron micrographs of Au-disk arrays prepared on GC (a) and on Pt (b) by the SECM microwriting approach using a RDP-A probe (a) and a RDP-B probe (b). Scale bars: 300 μm (a), 200 μm (b).

## 3. Results and discussion

### 3.1. Performance of the SECM-based microwriting procedure using RDP-A and RDP-B probes

Large arrays of reproducible gold microdisks as those shown in Fig. 3 were successfully fabricated both on GC (Fig. 3a) and on Pt (Fig. 3b) by the SECM-based microwriting procedure previously described, using both RDP-A and RDP-B probes, respectively. Arrays with up to 400 disks (20 × 20) were regularly obtained with good and repetitive morphological conditions of the disks. Consistent fabrication of arrays with more than 500 disks was only possible by using RDP-B tips. The effects of the sequence parameters and of the type of substrate on the spot morphology and on the array quality are summarized in Figs. 4–6 . The gold deposits become rougher when using more anodic $E_{T,dis}$ values, as it is shown in Fig. 4, and evidences of defects caused by bubbles are detected in

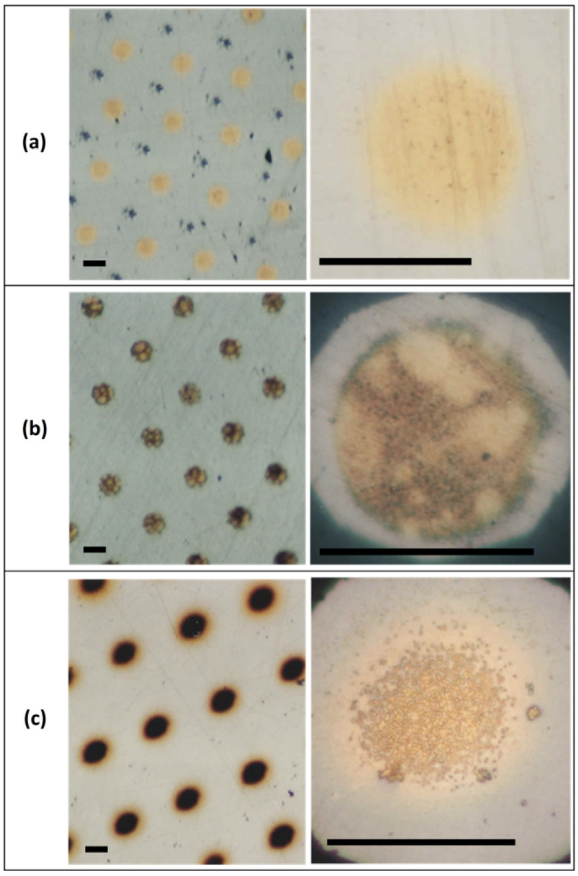


**Fig. 4.** Optical micrographs showing the effect of $E_{T,dis}$ on the morphology of Au disks deposited on GC using a RDP-A probe. $E_{T,dis}$ = 1.04 V (a), 1.08 V (b), 1.25 V (c) vs. SCE. Scale bars: 25 μm.

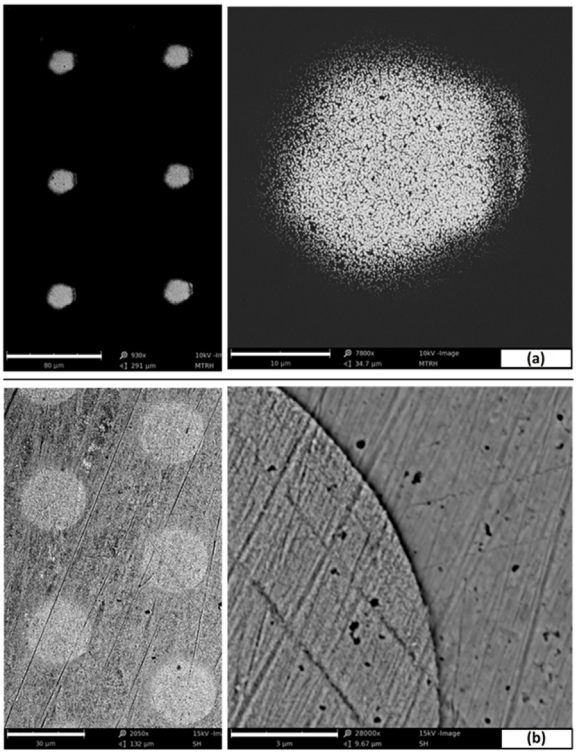


**Fig. 5.** Low (left) and high (right) magnification SEM micrographs of Au disks prepared on GC (a) and on Pt (b) by the SECM microwriting approach using a RDP-B type tip. $E_{T,dis}$ = 1.05 V vs. SCE; $t_{dis}$ = 2 s; $t_{dep}$ = 4 s. Scale bars: 80 μm (up left), 10 μm (up right), 30 μm (down left), 3 μm (down right).

some conditions (i.e. in Fig. 4b). The optimal condition to obtain arrays of flat spots for this low concentration of acid (0.1 M HCl) is by applying an $E_{T,dis}$ only slightly larger than the oxidation potential of Au (1.04 V vs. SCE) to avoid simultaneous gas evolution and an excessive local building of the $AuCl_4^-$ concentration. Differently to the previously reported metal patterns obtained by the microwriting method using conventional tips [23–26], in this case the deposited disks are well confined over a clearly delimited zone defined by the recessed disk shape. When using a 12.5-μm-radius tip and $t_{dis}$ = 2 s, granular deposits (denser at the disk center) as those shown in Fig. 5a are obtained on GC, and compact films with well-defined boundaries as those shown in Fig. 5b only result on Pt. The heterogeneous surface of glassy carbon provides reactive functionalized carbon sites randomly dispersed over a less active graphitic structure, which act as nucleation sites for electrodeposition, leading to the growth of isolated particles. Such behavior was already exploited by Mandler and co-workers to deposit ensembles of gold nano-crystals on different heterogeneous substrates [26,28,29], showing a strong influence of the operative conditions (electrolyte, pH, complexing agents) on the resulting morphology [26,28]. On the other hand, the polycrystalline Pt surface is more uniform in reactivity, leading to compact Au deposits. The thicknesses of the Au disks deposited on Pt measured by AFM were in the range 21 ± 3 nm. Under these conditions the integrated charge of Au dissolution on each step was 0.25 ± 0.02 μC, which leads to around $(8.6 \pm 0.7) \times 10^{-13}$ mol of dissolved $Au^{3+}$ (neglecting double layer and gas evolution charges). The density of Au atoms on the polycrystalline gold surface is $2.1 \times 10^{-9}$ mol cm$^{-2}$ [38], so a Au monolayer disk with 12.5-μm-radius should contain ~$10^{-14}$ mol of Au. This means that if all the dissolved $Au^{3+}$ is electrodeposited at the substrate as a 12.5-μm-radius disk of crystalline gold, then it should be composed by around 86 Au monolayers. A rough estimation of the deposited film thickness can be done taking into account the Au crystal structure (face centered cubic) and lattice constant (0.408 nm), which should result in a theoretical film of ~18 nm thickness, which is only slightly smaller than the value measured by AFM. On the other hand, the importance of a $t_{dep}$ value larger than $t_{dis}$ can be seen in Fig. 6. It is verified that the quiet time after dissolution ($t_{dep} > t_{dis}$) is particularly important when using RDP-B tips to prevent dispersion of dissolved gold and a deficient definition of the Au disks in the resulting array. This is because the transport of dissolved Au ions toward the substrate through the larger pipette inner volumes takes more time, which may cause

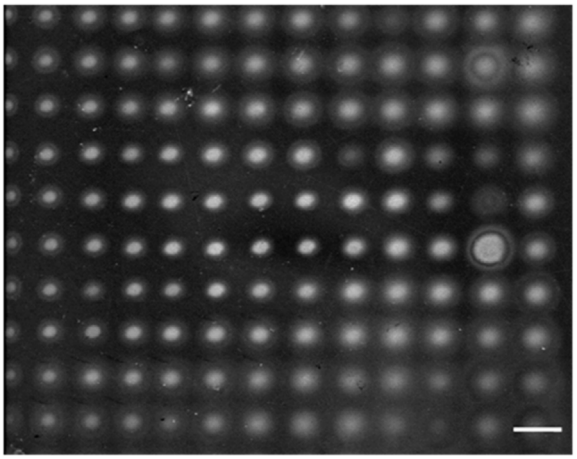

**Fig. 6.** SEM micrograph of a defective Au-disk array prepared on GC by the SECM microwriting approach using a RDP-B type tip and $t_{dep} = t_{dis}$. Scale bar: 50 μm.

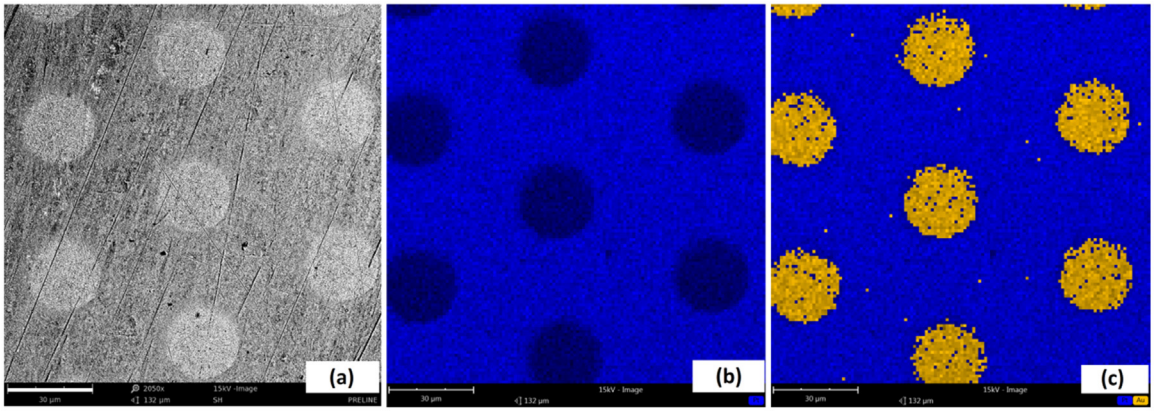


**Fig. 7.** SEM micrograph (a) and elemental mapping (b and c) of Pt (blue) and Au (yellow) of a Au-disk array prepared on Pt by the SECM microwriting approach using a RDP-B type tip. Scale bars: 30 μm. (For interpretation of the references to colour in this figure legend, the reader is referred to the web version of this article.)

dispersion of undeposited Au cations during tip displacement. The degree of confinement of the Au deposits was also evaluated. An elemental map of Au and Pt of a Au-disk array on a platinum substrate made with a RDP-B tip is shown in Fig. 7. Even though the characteristic X-ray energies of Pt and Au are very close and the Au film is relatively thin compared to the analysis deepness, the Au signals effectively come just from the deposited disks. Then, dispersed Au deposits, if any, are in amounts below the detection limit of this technique. Thus, it is verified that Au is well confined to the disk area, which is basically the area under the tip, as it is also observed in the disk boundary seen in Fig. 5b. Sizes and shapes of the resulting spots deposited on platinum substrates for both probe configurations are similar to those of the respective tip holes.

The recess in RDP-A probes is a key feature of the proposed method to obtain well defined and limited deposits. The surrounding inner wall acts directing current lines perpendicular to the surface and consequently minimizing the spot sizes. Nevertheless, as the array fabrication proceeds, the gap between gold disk and substrate increases. Thus for example, for a sequence with $t_{dis}$ = 2 s applied to a 12.5-μm-radius tip like the previously described with an etch rate of about 20 nm/disk, after 500 disks the tip would be etched a deepness of about 10 μm. Under these conditions the transfer process may become hampered by circumstantial effects (i.e. occluded gases or particles). In these conditions the configuration of RDP-B tip becomes advantageous, because it allows a continuous renovation of the metal source since the compression system keeps the gold wire in the same position during the array fabrication. Thus, this last configuration enables the fabrication of larger (and/or denser) arrays, although longer quiet times ($t_{dep} >> t_{dis}$) are required to prevent Au dispersion and to attain a better confined deposit, which results in much longer times for fabrication of the whole arrays.

### 3.2. Mechanical stability

As can be seen in Fig. 8a, SEM evaluation of the GC-supported Au arrays that were subjected to the hydrodynamic test shows almost no morphological variations respect to the unused ones (as that shown in Fig. 5a). Differences are only caused by some particles from the solution that remained stuck on the surface after rotation. A similar result was obtained with Pt-supported Au arrays. Moreover, the CVs of these last arrays before and after the hydrodynamic test are shown in Fig. 8b, where the voltammetric features of Pt and Au (peaks for electro-oxidation, oxide reduction, and H electro-adsorption on Pt) can be clearly observed. In the CVs of the unused array, there is a clear inhibition (affecting mostly the electro-oxidation charges and the peaks of H electro-adsorption on Pt), which is probably caused by adsorbed chloride that remained from the deposition solution. The charges of these surface processes on the rotated array resulted in fact slightly larger than those measured on the unused array, both for Pt and Au. This indicates not only that there is no loose of material during rotation but also that the electrode surface is cleaned. On the basis of these evidences, it is concluded that these arrays are mechanically stable even under the hardest hydrodynamic conditions found in electrochemical experiments.

### 3.3. Selective modification of Au-disk arrays

In order to exemplify possible ways to use these arrays as supports of catalytic materials for a specific task, Au-disk array were modified with Pt ad-layers by deposition of UPD Cu and redox replacement, as described previously. Fig. 9 shows elemental mapping results of Pt, Au and C on a Au-disk array deposited on GC uniformly modified with Pt. Gold and platinum are only detected over the spots, indicating that Cu UPD deposition proceeds only on the Au disks, and no detectable spontaneous Pt deposition is verified on GC during the redox replacement step. Besides, traces of Cu were not detected by this technique. Thus, it is demonstrated that the modification of Au arrays by UPD Cu and further redox replacement by Pt is a feasible method that can be implemented for using the arrays as platforms for selective modification with other components.

### 3.4. SECM screening of activity for hydrogen evolution on Pt-modified Au-disk arrays

The electrocatalytic activity for hydrogen evolution of Pt-modified Au-disk arrays deposited on GC was evaluated by SECM imaging in the SG-TC mode in 0.5 M $H_2SO_4$, as previously described. On uniformly modified arrays this screening pointed to visualize the recurrence of the same hydrogen evolution response on each different spot at a given potential, as this should be proportional to the Pt coverage [37] (which should repeat on each spot). A typical SECM image can be seen in Fig. 10. Slight variations over the range 42 − 47 nA are observed in the tip current values registered at the centers of the imaged disks, which indicate variations of the local concentrations of electrogenerated hydrogen between roughly 1.2 and 1.4 mM (calculated from the current for a disk microelectrode [30]). These are small differences that can be caused either by a slight drift of the tip-substrate distance due to substrate tilt, or by small changes of the gold roughness among disks. Thus, the activity for hydrogen evolution verified on the spots at a fixed potential is comparable, indicating a reproducible modification of spots with similar amounts of Pt.

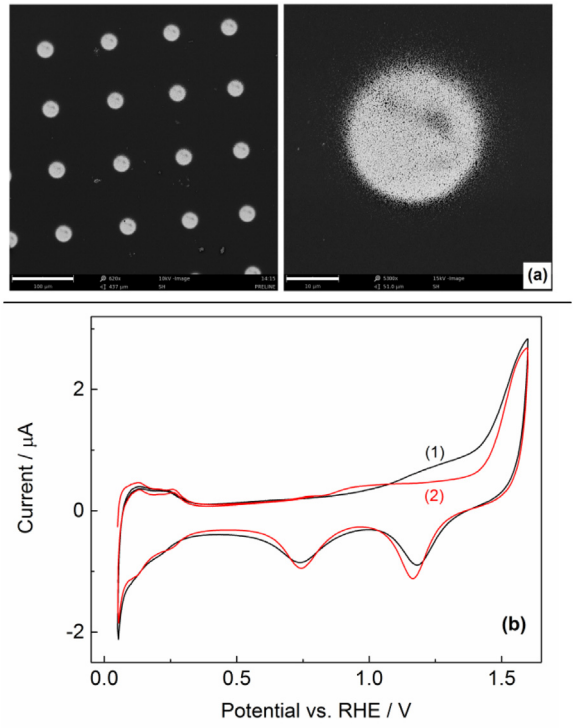


**Fig. 8.** (a) SEM micrographs of a GC-supported Au-disk array after the hydrodynamic test. Scale bars: 100 µm (left), 10 µm (right). (b) Cyclic voltammograms in 0.5 M $H_2SO_4$ of a Pt-supported Au-disk array before (1) and after (2) the hydrodynamic test.

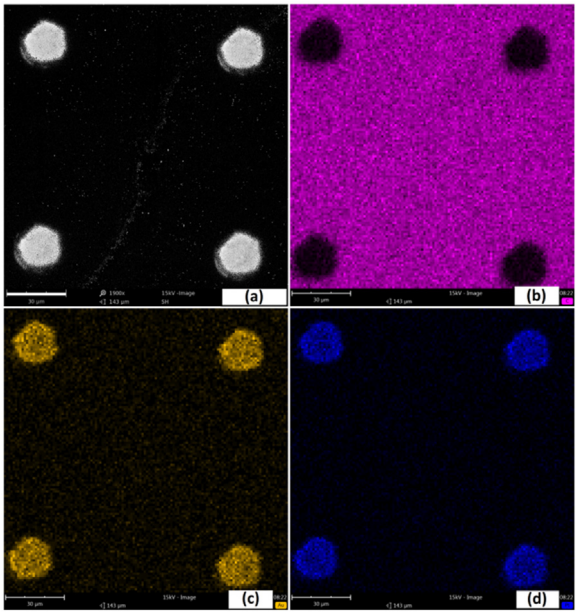


**Fig. 9.** SEM micrograph (a) and elemental mapping of C (b), Au (c), and Pt (d) of Pt-modified Au disks deposited on GC by the SECM microwriting approach using a RDP-B type tip. Scale bars: 30 µm.

## 4. Conclusions

The SECM-based microwriting method can be applied through well-coordinated steps involving electro-dissolution, electrodeposition, resting, lifting, approaching and displacement periods, for successful fabrication of extensive arrays of Au disks with more than 400 disks. Recessed microdisk tips were employed, placing

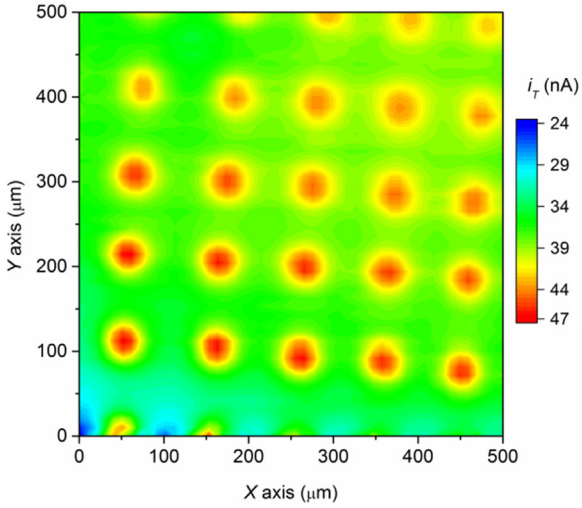


**Fig. 10.** SECM SG-TC image of activity for hydrogen evolution on a Au-disk array modified with Pt on GC, in 0.5 M $H_2SO_4$. Tip: Pt, 12.5 µm-radius. Scan rate: 100 µm/s. $E_T$ = 0.4 V vs. RHE, $E_S$ = −0.05 V vs. RHE.

them in slight contact with the substrate surface to generate a mobile gap between the microelectrode source and the substrate. These tips resulted to be key components to attain such large arrays of reproducible and well-defined disks. Two types of recessed probes were successfully employed. One was a typical Au disk tip slightly etched, while the other was a micropipette housing at its inner end a gold wire pressed against its opening leaving a gap of a few microns. The first one showed very good performance to obtain arrays containing no more than 400 disks in a relatively shorter time (~30 min), and the second one was useful when even larger arrays were required, involving larger preparation times. The inclusion in the fabrication program of quiet (or resting) periods was another key aspect of the method to ensure good confinement and repeatability of the electrodeposited disks. The proposed strategy is also useful for other SECM microfabrication modes (e.g. etching, micromachining). Moreover, a similar fabrication approach using the developed probes and the proposed sequence of steps could be applied, on the basis of reported studies with conventional tips, to obtain arrays on other types of substrates such as insulating surfaces (either by inducing local electroless deposition [28] or local etching of metallic [39], oxide [21], or organic [40] masks).

The apparent limitations of the method (as compared with other microfabrication approaches) are mainly associated with the resolution, the writing speed, and the cost of the required facilities. In fact the low resolution is inherent to the simple setup that was used in this work. If a better resolution is required, the same strategy can be applied using smaller probes and a positioning system based on piezo-translators (instead of stepper motors). Further developments pointing to increase the resolution to a nanometer level should also involve the addition of an independent mechanism for controlling the tip position in order to prevent crashing of the fragile submicrometer-sized probes. On the other hand, the relatively low writing speed is an issue that in some cases may result inconvenient, but in fact most of the fabrication time is spent during the spotting process, which is automatic and no attention of the operator is required at all. Regarding to the involved costs, it is not simple to compare how expensive the method is against others, as it depends on many factors including the usual facilities of the user. A basic microwriting arrayer is not very expensive, since the most complex involved instrument is a potentiostat. For laboratories with basic electrochemical instrumentation this method could be advantageous against others, as an XYZ positioning stage can be easily mounted using stepper motors (even those from printers or

plotters). Of course, increasing resolution will require more precise instrumentation that will make the setup more expensive.

The fabricated arrays have numerous applications in varied electrochemical areas. For example, we showed that Au disks deposited on glassy carbon can be selectively modified with other metal, in this case by adsorption of UPD Cu and further exchange with Pt (or another noble metal). In this work these arrays were used as platforms to sense the electrocatalytic activity of Pt-modified Au disks for the hydrogen evolution reaction by SECM. Other methods to selectively activate Au as a support for other materials (for example by adsorption of self-assembled monolayers [41]) can also be used on this type of arrays.

The potential applications of the SECM-based micromachining technologies obviously extend much beyond just the fabrication of arrays. The capability of SECM to monitor the surface topography/reactivity and to simultaneously induce a local modification of the surface opens up many unique possibilities for the design of electrochemical experiments. For example, an electrode with arbitrary shape can be deposited from a SECM tip right next to a selected single unity (e.g. a cell or a nanoparticle) that was previously located by the same SECM probe. This electrode can be used to induce a local chemical perturbation that causes a response of the studied single system, which is detected by the SECM tip. Such strategy can be used to improve the control of SECM studies of metabolic processes on cells [42,43], catalysis, electrocatalysis, and photocatalysis on nanoparticles [44–46], among many other systems. The application of this technique for modification of well-defined surfaces with tip-generated species (e.g. decoration of monocrystalline planes with metal ad-atoms [47], local attachment of specific moieties on modified surfaces [48–51]) followed by *in situ* evaluation would also be viable.

## Aknowledgements

This work was supported by Agencia Nacional de Promoción Científica y Tecnológica (PICT 2014 2001, PICT-E 2014 0239), Consejo Nacional de Investigaciones Científicas y Técnicas (PIP 112-201101-00674) and Universidad Nacional del Litoral (CAI + D 501-201101-00333 LI). The authors thank Dr. A.C. Chialvo for his valuable suggestions.

## References

[1] C.N. LaFratta, D.R. Walt, Very high density sensing arrays, Chem. Rev. 108 (2008) 614.
[2] O. Ordeig, J. del Campo, F.X. Munoz, C.E. Banks, R.G. Compton, Electroanalysis utilizing amperometric microdisk electrode arrays, Electroanalysis 19 (2007) 1973.
[3] R. Feeney, S.P. Kounaves, Microfabricated ultramicroelectrode arrays: developments, advances, and applications in environmental analysis, Electroanalysis 12 (2000) 677.
[4] V. Scognamiglio, I. Pezzotti, G. Pezzotti, J. Cano, I. Manfredonia, K. Buonasera, G. Rodio, M.T. Giardi, A new embedded biosensor platform based on micro-electrodes array (MEA) technology, Sens. Actuators B 176 (2013) 275.
[5] Y.K. Wang, Z.L. Wang, M.S. Li, W.L. Zeng, M.H. Weng, Microelectrode array fabrication by micro-WEDM, Adv. Mater. Res. 69–70 (2009) 79.
[6] C. Yue, Y. Yu, J. Yin, T. Wong, Y. Zang, J. Li, J. Kang, Fabrication of 3D hexagonal bottle-like Si-SnO2 core-shell nanorod arrays as anode material in on chip micro-lithium-ion-batteries, J. Mater. Chem. A 1 (2013) 7896.
[7] J.L. Fernández, D.A. Walsh, A.J. Bard, Thermodynamic guidelines for the design of bimetallic catalysts for oxygen electroreduction and rapid screening by scanning electrochemical microscopy. M-Co (M: Pd Ag, Au), J. Am. Chem. Soc. 127 (2005) 357.
[8] F. Zhang, V. Roznyatovskiy, F.-R.F. Fan, V. Lynch, J.L. Sessler, A.J. Bard, A method for rapid screening of photosensitizers by scanning electrochemical microscopy (SECM) and the synthesis and testing of a porphyrin sensitizer, J. Phys. Chem. C 115 (2011) 2592.
[9] D. Menshykau, F.J. del Campo, F.X. Muñoz, R.G. Compton, Current collection efficiency of micro- and nano-ring-recessed disk electrodes and of arrays of these electrodes, Sens. Actuators B 138 (2009) 362.
[10] N. Godino, X. Borrisé, F.X. Muñoz, F.J. del Campo, R.G. Compton, Mass transport to nanoelectrode arrays and limitations of the diffusion domain approach: theory and experiments, J. Phys. Chem. C 113 (2009) 11119.
[11] G.C. Luque, M.R. Gennero de Chialvo, A.C. Chialvo, Intermetallic junction contribution to the CO electrooxidation on a Pt/Au electrode: the excess voltammetric current, J. Solid State Electrochem. 20 (2015) 1209.
[12] C.G. Zoski, N. Simjee, O. Guenat, M. Koudelka-Hep, Addressable microelectrode arrays: characterization by imaging with scanning electrochemical microscopy, Anal. Chem. 76 (2004) 62.
[13] S. Partel, S. Kasemann, P. Choleva, C. Dincer, J. Kieninger, G.A. Urban, Novel fabrication process for sub-micron interdigitated electrode arrays for highly sensitive electrochemical detection, Sens. Actuators B 205 (2014) 193.
[14] Y.H. Lanyon, D.W.M. Arrigan, Recessed nanoband electrodes fabricated by focused ion beam milling, Sens. Actuators B 121 (2007) 341.
[15] S. Rauf, M.J.A. Shiddiky, A. Asthana, K. Dimitrov, Fabrication and characterization of gold nanohole electrode arrays, Sens. Actuators B 173 (2012) 491.
[16] B.-R. Maeng, K.-T. Nam, S.-K. Lee, J.-H. Park, Fabrication and measurement of microtip electrode array with self-aligned integrated dual conductive electrodes, Sens. Actuators B 237 (2016) 1015.
[17] O. Schneegans, A. Moradpour, F. Houzé, A. Angelova, C. Henry de Villeneuve, P. Allongue, P. Chrétien, Conducting probe-mediated electrochemical nanopatterning of molecular materials, J. Am. Chem. Soc. 123 (2001) 11486.
[18] F. Chen, H. Jiang, A.M. Kiefer, A.M. Clausen, Y.-H. Ting, A.E. Wendt, B. Ding, M.G. Lagally, Fabrication of ultrahigh-density nanowires by electrochemical nanolithography, Nanoscale Res. Lett. 6 (2011) 444.
[19] T.M. Braun, D.T. Schwartz, Localized electrodeposition and patterning using bipolar electrochemistry, J. Electrochem. Soc. 162 (2015) D180.
[20] Y.-J. Ciou, Y.-R. Hwang, J.-C. Lin, Y.-T. Tseng, Fabrication of 3D microstructures by localized electrochemical deposition with image feedback distance control and five-axis motion platform, ECS J. Solid State Sci. Technol. 5 (2016) P425.
[21] D. Battistel, S. Daniele, D. Fratter, A scanning electrochemical microscopy procedure for micropatterning Al2O3-thin films deposited on a platinum substrate, Electrochim. Acta 78 (2012) 557.
[22] Y.-M. Wuu, F.-R.F. Fan, A.J. Bard, High resolution deposition of polyaniline on Pt with the scanning electrochemical microscope, J. Electrochem. Soc. 136 (1989) 885.
[23] D. Mandler, Micro- and nanopatterning using scanning electrochemical microscopy, in: A.J. Bard, M.V. Mirkin (Eds.), Scanning Electrochemical Microscopy, 2nd ed., CRC Press, Boca Raton, 2012, pp. 489–524.
[24] M. Sheffer, D. Mandler, Scanning electrochemical imprinting microscopy: a tool for surface patterning, J. Electrochem. Soc. 155 (2008) D203.
[25] S. Meltzer, D. Mandler, Microwriting of gold patterns with the scanning electrochemical microscope, J. Electrochem. Soc. 142 (1995) L82.
[26] E. Ammann, D. Mandler, Local deposition of gold on silicon by the scanning electrochemical microscope, J. Electrochem. Soc. 148 (2001) C533.
[27] O. de Abril, D. Mandler, P.R. Unwin, Local cobalt electrodeposition using the scanning electrochemical microscope, Electrochem. Solid State Lett. 7 (2004) C71.
[28] E. Malel, D. Mandler, Localized electroless deposition of gold nanoparticles using scanning electrochemical microscopy, J. Electrochem. Soc. 155 (2008) D459.
[29] E. Malel, R. Ludwig, L. Gorton, D. Mandler, Localized deposition of Au nanoparticles by direct electron transfer through cellobiose dehydrogenase, Chem. Eur. J. 16 (2010) 11697.
[30] H.L. Bonazza, J.L. Fernández, An efficient method for fabrication of disk-shaped scanning electrochemical microscopy probes with small glass-sheath thicknesses, J. Electroanal. Chem. 650 (2010) 75.
[31] F.F. Fan, J.L. Fernández, B. Liu, J. Mauzeroll, C.G. Zoski, UME fabrication/characterization basis, in: C.G. Zoski (Ed.), Handbook of Electrochemistry, Elsevier, Amsterdam, 2007, pp. 189–197.
[32] D.A. Walsh, J.L. Fernández, J. Mauzeroll, A.J. Bard, Scanning electrochemical microscopy. 55. Fabrication and characterization of micropipet probes, Anal. Chem 77 (2005) 5182.
[33] T. Ohshiro, T. Ito, P. Bühlmann, Y. Umezawa, Scanning tunneling microscopy with chemically modified tips: discrimination of porphyrin centers based on metal coordination and hydrogen bond interactions, Anal. Chem. 73 (2001) 878.
[34] P. Sun, M.V. Mirkin, Scanning electrochemical microscopy with slightly recessed nanotips, Anal. Chem. 79 (2007) 5809.
[35] Y. Yu, Y. Hu, X. Liu, W. Deng, X. Wang, The study of Pt@Au electrocatalyst based on Cu underpotential deposition and Pt redox replacement, Electrochim. Acta 54 (2009) 3092.
[36] F.F. Fan, J.L. Fernández, B. Liu, J. Mauzeroll, Scanning electrochemical microscopy, in: C.G. Zoski (Ed.), Handbook of Electrochemistry, Elsevier, Amsterdam, 2007, pp. 471–540.
[37] M.A. Brites Helú, M.R. Gennero de Chialvo, A.C. Chialvo, J.L. Fernández, Nanoparticle ensemble electrodes: fabrication by short-pulse sputtering and characterization by scanning probe microscopy and voltammetry, J. Solid State Electrochem. 18 (2014) 2233.
[38] H. Angerstein-Kozlowska, B.E. Conway, A. Hamelin, L. Stoicoviciu, Elementary steps of electrochemical oxidation of single-crystal planes of Au—I. Chemical basis of processes involving geometry of anions and the electrode surfaces, Electrochim. Acta 31 (1986) 1051.
[39] M. Sheffer, D. Mandler, Why is copper locally etched by scanning electrochemical microscopy? J. Electroanal. Chem. 622 (2008) 115.

[40] N. Ktari, C. Combellas, F. Kanoufi, Local oxidation of polystyrene by scanning electrochemical microscopy, J. Phys. Chem. C 115 (2011) 17891.
[41] J. Clausmeyer, W. Schuhmann, N. Plumeré, Electrochemical patterning as a tool for fabricating biomolecule microarrays, Trends Anal. Chem. 58 (2014) 23.
[42] J. Mauzeroll, A.J. Bard, O. Owhadian, T.J. Monks, Menadione metabolism to thiodione in hepatoblastoma by scanning electrochemical microscopy, Proc. Natl. Acad. Sci. U. S. A. 101 (2004) 17582.
[43] J.P. Wilburn, M. Ciobanu, D.E. Cliffel, Scanning electrochemical microscopy of individual pancreatic islets, J. Electrochem. Soc. 163 (2016) H3077.
[44] M.A. OíConnell, J.R. Lewis, A.J. Wain, Electrochemical imaging of hydrogen peroxide generation at individual gold nanoparticles, Chem. Commun. 51 (2015) 10314.
[45] J. Kim, C. Renault, N. Nioradze, N. Arroyo-Currás, K.C. Leonard, A.J. Bard, Electrocatalytic activity of individual Pt nanoparticles studied by nanoscale scanning electrochemical microscopy, J. Am. Chem. Soc. 138 (2016) 8560.
[46] D. Yuan, L. Zhan, J. Lai, L. Xie, B. Mao, D. Zhan, SECM evaluations of the crystal-facet-correlated photocatalytic activity of hematites for water splitting, Electrochem. Commun. 73 (2016) 29.
[47] B.D.B. Aaronson, S.C.S. Lai, P.R. Unwin, Spatially resolved electrochemistry in ionic liquids: surface structure effects on triiodide reduction at platinum electrodes, Langmuir 30 (2014) 1915.
[48] S. Lhenry, Y.R. Leroux, C. Orain, F. Conan, N. Cosquer, N. Le Poul, O. Reinaud, Y. Le Mest, P. Hapiot, Locally induced and self-induced electroclick onto a self-assembled monolayer: writing and reading with SECM under unbiased conditions, Langmuir 30 (2014) 4501.
[49] D. Quinton, A. Maringa, S. Griveau, T. Nyokong, F. Bedioui, Surface patterning using scanning electrochemical microscopy to locally trigger a click chemistry reaction, Electrochem. Commun. 31 (2013) 112.
[50] L. Stratmann, J. Clausmeyer, W. Schuhmann, Non-destructive patterning of carbon electrodes by using the direct mode of scanning electrochemical microscopy, ChemPhysChem 16 (2015) 3477.
[51] A.N. Patel, K. McKelvey, P.R. Unwin, Nanoscale electrochemical patterning reveals the active sites for catechol oxidation at graphite surfaces, J. Am. Chem. Soc. 134 (2012) 20246.

## Biographies

**Mariela A. Brites Helú** received her B.S. degree in 2013 from the Facultad de Ingeniería Química, Universidad Nacional del Litoral (Argentina). Currently she is studying for her Ph.D. degree in Chemistry at the same institution. Her research interest is focused on applications of scanning electrochemical microscopy in electrocatalysis.

**José L. Fernández** received his B.S. degree in Chemistry in 1996 from the Universidad Nacional del Litoral (Argentina), followed by a PhD degree in Chemistry in 2001 at the same institution. He was a postdoctoral researcher (2002–2005) at the Department of Chemistry and Biochemistry of The University of Texas at Austin. Currently he is a Professor at the Facultad de Ingeniería Química, Universidad Nacional del Litoral, and a CONICET Researcher. His research interest is focused on the development and application of micro-electrochemical methods on fundamental and applied issues related to energy conversion processes.